Available online at www.sciencedirect.com
SCIENCE DIRECT®
Journal of Computational Physics 211 (2006) 1–8
JOURNAL OF COMPUTATIONAL PHYSICS
www.elsevier.com/locate/jcp

Short Note

The method of fundamental solutions for 2D and 3D Stokes problems

D.L. Young [a,*], S.J. Jane [a], C.M. Fan [a], K. Murugesan [a], C.C. Tsai [b]

[a] *Department of Civil Engineering and Hydrotech Research Institute, National Taiwan University, Taipei, Taiwan*
[b] *Department of Information Technology, Toko University, Chia-Yi County, Taiwan*

Received 9 January 2004; received in revised form 13 May 2005; accepted 25 May 2005
Available online 12 July 2005

Abstract

A numerical scheme based on the method of fundamental solutions (MFS) is proposed for the solution of 2D and 3D Stokes equations. The fundamental solutions of the Stokes equations, Stokeslets, are adopted as the sources to obtain flow field solutions. The present method is validated through other numerical schemes for lid-driven flows in a square cavity and a cubic cavity. Test results obtained for a rectangular cavity with wave-shaped bottom indicate that the MFS is computationally efficient than the finite element method (FEM) in dealing with irregular shaped domain. The paper also discusses the effects of number of source points and their locations on the numerical accuracy.

Keywords: Stokes flows; The method of fundamental solutions; Stokeslets; 2D and 3D flows

1. Introduction

The MFS free from meshes, singularities, and numerical integrations is one of the promising meshless numerical schemes for solving partial differential equations (PDEs). The basic concept of MFS is to decompose the solutions of the given PDEs by superposition of the fundamental solutions with proper intensities, which are not known a priori. These intensities are determined by collocating the known field points on the boundary. Some excellent reviews on the MFS highlighting its advantages over the domain discretization numerical schemes are available in [1,2]. The MFS first proposed by Kupradze and Aleksidze [3] has been widely used in the numerical solutions for the Laplace, Poisson, biharmonic, Helmholtz and diffusion equations. As far as its applications to flow problems are concerned, only Stokes equations have been attempted.

* Corresponding author. Fax: +886 2 23626114.
E-mail address: dlyoung@ntu.edu.tw (D.L. Young).

0021-9991/$ - see front matter
doi:10.1016/j.jcp.2005.05.016

For 2D flows, one approach is to transform the Stokes equations into the biharmonic equations using the stream function formulation [4]. Another approach is to recast the Stokes equations in velocity–vorticity form, thus resulting in the Laplace equation and Poisson equation [5]. Both are then finally solved by the MFS. Those two approaches will have no immediate solutions of the pressure.

The Stokeslets have already been employed in the boundary element method (BEM) for the solution of Stokes flows [6]. In the present work, the MFS based on the Stokeslets is developed to directly solve the Stokes equations for all the field variables. The Stokeslets represent the flow fields due to concentrated point forces. Hence, when the Stokeslets are used as field intensities called source points in the MFS, the physics underlying the Stokes problems can be easily satisfied. Numerical works on 2D Stokes flows carried out by Alves and Silvestre [7], Young et al. [8] and Chen et al. [9] focused only on regular geometries. The present work extends the application of the MFS to 2D irregular geometry and 3D application. The accuracy and efficiency of the present numerical scheme are demonstrated by means of validation results for a square cavity and a cubic cavity and a test problem for a rectangular cavity with wave-shaped bottom. Since the location of the source points is an important issue on the convergence in the MFS solution procedures, an analysis is performed to study the effects of the number of source points and their locations on the numerical accuracy.

2. Governing equations and Stokeslets

The Stokes equations for an incompressible flow can be represented by the continuity and momentum equations as:

$$\nabla \cdot \vec{u} = 0, \tag{1}$$

$$-\nabla p + \mu \nabla^2 \vec{u} = 0, \tag{2}$$

where $\vec{u} = (u, v, w)$ is the velocity vector, p is the pressure and μ is the dynamic viscosity. The vorticity is another important physical variable and is expressed as $\vec{\omega} = \nabla \times \vec{u}$, where $\vec{\omega} = (\omega_x, \omega_y, \omega_z)$ is the vorticity vector. For two-dimensional flow, the stream function ψ is defined by $u = \frac{\partial \psi}{\partial y}$ and $v = -\frac{\partial \psi}{\partial x}$.

The fundamental solutions for the Stokes operators are called the Stokeslets, which represent the flow fields due to concentrated point forces. The Stokeslets for two-dimensional flow can be obtained as [6]:

$$u^* = \frac{1}{8\pi\mu}\left[\alpha^x\left(-2\ln(r) + \frac{2(x-x_0)^2}{r^2} - 3\right) + \alpha^y\left(\frac{2(x-x_0)(y-y_0)}{r^2}\right)\right], \tag{3a}$$

$$v^* = \frac{1}{8\pi\mu}\left[\alpha^x\left(\frac{2(x-x_0)(y-y_0)}{r^2}\right) + \alpha^y\left(-2\ln(r) + \frac{2(y-y_0)^2}{r^2} - 3\right)\right], \tag{3b}$$

$$p^* = \frac{1}{2\pi}\left[\alpha^x\left(\frac{(x-x_0)}{r^2}\right) + \alpha^y\left(\frac{(y-y_0)}{r^2}\right)\right], \tag{3c}$$

$$\psi^* = \frac{1}{8\pi\mu}\left[\alpha^x(-2(y-y_0)\ln(r) - (y-y_0)) + \alpha^y(2(x-x_0)\ln(r) + (x-x_0))\right], \tag{3d}$$

where $r = |\vec{x} - \vec{x}_0|$ is the distance between a field point $\vec{x}$ and a source point $\vec{x}_0$. Similarly, the Stokeslets for three-dimensional flow can be obtained as [6]:

$$u^* = \frac{1}{8\pi\mu}\left[\alpha^x\left(-\frac{1}{r} - \frac{(x-x_0)^2}{r^3}\right) + \alpha^y\left(-\frac{(x-x_0)(y-y_0)}{r^3}\right) + \alpha^z\left(-\frac{(x-x_0)(z-z_0)}{r^3}\right)\right], \tag{4a}$$

$$v^* = \frac{1}{8\pi\mu}\left[\alpha^x\left(-\frac{(x-x_0)(y-y_0)}{r^3}\right) + \alpha^y\left(-\frac{1}{r} - \frac{(y-y_0)^2}{r^3}\right) + \alpha^z\left(-\frac{(y-y_0)(z-z_0)}{r^3}\right)\right], \tag{4b}$$

$$w^* = \frac{1}{8\pi\mu}\left[\alpha^x\left(-\frac{(x-x_0)(z-z_0)}{r^3}\right) + \alpha^y\left(-\frac{(y-y_0)(z-z_0)}{r^3}\right) + \alpha^z\left(-\frac{1}{r} - \frac{(z-z_0)^2}{r^3}\right)\right], \tag{4c}$$

$$p^* = \frac{1}{4\pi}\left[\alpha^x\left(\frac{(x-x_0)}{r^3}\right) + \alpha^y\left(\frac{(y-y_0)}{r^3}\right) + \alpha^z\left(\frac{(z-z_0)}{r^3}\right)\right]. \tag{4d}$$

The applied point forces $\vec{\alpha} = (\alpha^x, \alpha^y, \alpha^z)$ take their magnitudes after satisfying the boundary conditions at the selected number of collocation points. This is part of the numerical procedure in the MFS and will be discussed in the following section.

3. MFS formulations

According to the principles of the MFS the velocity field can be obtained using the corresponding Stokeslets in Eqs. (3a) and (3b):

$$u(\vec{x}_i) = \frac{1}{8\pi\mu}\left[\sum_{j=1}^{N}\alpha_j^x\left(-2\ln(r_{ij}) + \frac{2(x_i-\xi_j)^2}{r_{ij}^2} - 3\right) + \sum_{j=1}^{N}\alpha_j^y\left(\frac{2(x_i-\xi_j)(y_i-\eta_j)}{r_{ij}^2}\right)\right], \tag{5a}$$

$$v(\vec{x}_i) = \frac{1}{8\pi\mu}\left[\sum_{j=1}^{N}\alpha_j^x\left(\frac{2(x_i-\xi_j)(y_i-\eta_j)}{r_{ij}^2}\right) + \sum_{j=1}^{N}\alpha_j^y\left(-2\ln(r_{ij}) + \frac{2(y_i-\eta_j)^2}{r_{ij}^2} - 3\right)\right], \tag{5b}$$

where N is the number of source points and α_j^x and α_j^y are the undetermined coefficients that represent the strengths of singularities in the x- and y-directions, respectively; $\vec{x}_i = (x_i, y_i)$ is the position of the field point; $\vec{s}_j = (\xi_j, \eta_j)$ is the location of the source point and $r = |\vec{x}_i - \vec{s}_j|$ is the distance between a field point and a source point. The boundary conditions of the velocity components will be collocated for certain field points on the boundary in order to determine the unknown coefficients (α_j^x, α_j^y). In this work, for simplicity we typically select the source points close to the boundary as illustrated in Fig. 1, and assume that the number of source points is equal to the number of boundary field points so that the method of collocation can be used. Once the coefficients are computed, all the field variables can be obtained directly by taking summation over the source points outside the computational domain from Eqs. (5a), (5b), (6a) and (6b):

$$p(\vec{x}_i) = \frac{1}{2\pi}\left[\sum_{j=1}^{N}\alpha_j^x\left(\frac{x_i-\xi_j}{r^2}\right) + \sum_{j=1}^{N}\alpha_j^y\left(\frac{y_i-\eta_j}{r^2}\right)\right], \tag{6a}$$

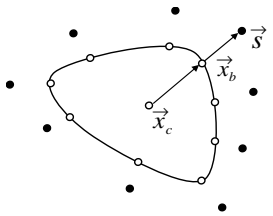

Fig. 1. Schematic diagram of the distribution of source and boundary field points. $\vec{s} = \vec{x}_b + b(\vec{x}_b - \vec{x}_c)$. ($\vec{s}$: location of source point, $\vec{x}_b$: location of boundary field point, $\vec{x}_c$: center).

$$\psi(\vec{x}_i) = \frac{1}{8\pi\mu}\left[\sum_{j=1}^{N}\alpha_j^x(-2(y_i-\eta_j)\ln(r_{ij}) - (y_i-\eta_j)) + \sum_{j=1}^{N}\alpha_j^y(2(x_i-\xi_j)\ln(r_{ij}) + (x_i-\xi_j))\right]. \quad (6b)$$

By adopting a similar procedure we can obtain the flow field variables for the 3D Stokes equations.

The proper location of the source points is an important issue in the MFS with respect to the accuracy of the numerical solution. In this paper, the position of the source points in computational domain is computed by the following equation:

$$\vec{s} = \vec{x}_b + b(\vec{x}_b - \vec{x}_c), \quad (7)$$

where $\vec{s} = (\xi, \eta, \zeta)$ is the spatial coordinates of the source point, $\vec{x}_b = (x_b, y_b, z_b)$ is the spatial coordinates of the boundary field point, $\vec{x}_c = (x_c, y_c, z_c)$ is the spatial coordinates of the center of the computational domain and b is a spatial parameter. Once the parameter b is chosen, the distribution of the source points is determined.

4. Results and discussions

The proposed numerical scheme is validated by solving 2D and 3D Stokes equations in a lid-driven square cavity, a rectangular cavity with wave-shaped bottom and a cubic cavity.

4.1. Square cavity

Stokes flow in a square cavity with the top lid moving with a unit velocity in the horizontal x-direction is considered as the first validation problem. The predicted results for u–y and x–v plots are compared with the solutions of non-singular boundary integral equation method (NSBIEM) [10] and multiquadrics method (MQ) [11] as shown, respectively, in Fig. 2(a) and (b). To study the effect of number of boundary field points on the numerical accuracy, the MFS results obtained with 44, 72 and 80 boundary field points are depicted in Fig. 2(a). As the number of boundary field points increases from 44 to 80, the present predictions approach and coincide with the results of NSBIEM [10] and MQ [11]. The effect of the position of source locations, obtained using Eq. (7), on the

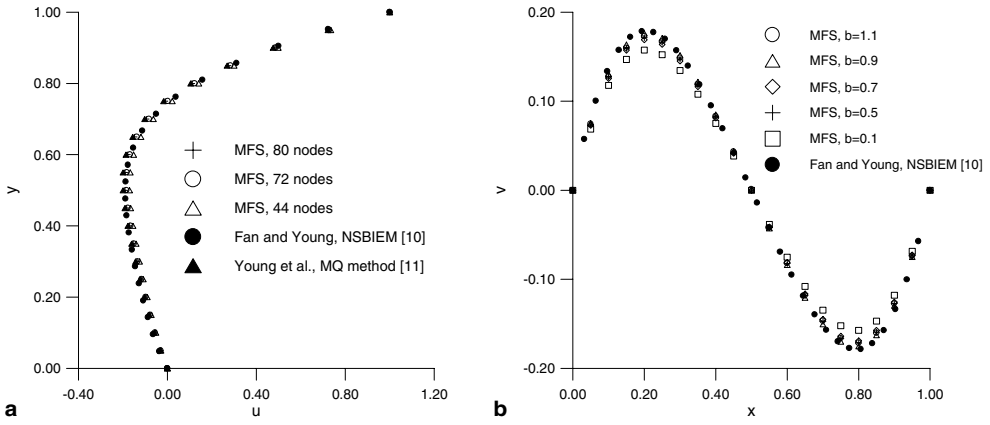

Fig. 2. (a) Comparison of u velocity profile along y at $x = 0.5$ for a square cavity (b) Comparison of v velocity profile along x at $y = 0.5$ with different source point locations ($N = 80$) for a square cavity.

numerical accuracy of the MFS is also investigated and the results are compared for the x–v plot as shown in Fig. 2(b). It is observed that accurate numerical results could be obtained for a given interior field point, when the source points are located off the boundary at about 90% of the distance from the center. With regard to the ill-conditioning of the matrix equations generally observed in the MFS, our numerical experiments indicate that the resulting simultaneous equations are not ill-conditioned, when the value of the spatial parameter b is considered in the range from 0.1 to 1.1. Beyond this range the equations are found to be ill-conditioned.

4.2. Rectangular cavity with wave-shaped bottom

The capability of the proposed numerical scheme to handle irregular computational domains is demonstrated by solving a lid-driven rectangular cavity with wave-shaped bottom. Since analytic solutions for such a complex geometry are not available, initially the problem was solved using the FEM with 6000 bilinear elements and 6161 grid points. Fig. 3 shows the comparison of results for u–y plot obtained by the FEM and MFS using 280, 420 and 560 boundary field points. The results predicted by the MFS are in close agreement with the FEM solutions. It is observed that when the spatial parameter b in Eq. (7) is assumed as 0.1, the numerical accuracy of the MFS results is insensitive to the number of boundary field points considered in the above range, and further the matrix equations are not ill-conditioned. It should be noted that for simulating the flow field in this irregular shape domain, the MFS requires only 560 boundary nodes as compared to 6161 grid points by the FEM. This demonstrates that the MFS is found to be computationally efficient to handle the irregular shaped domains. Figs. 4(a)–(d) depict the distributions of velocity vector, vorticity, pressure and streamlines, respectively. The vorticity is computed from the velocity field using the vorticity definition. The numerical results indicate that the flow symmetry pattern still remains as expected for the Stokes flow. However, the flow pattern gets modified in accordance with the irregular boundary of the domain.

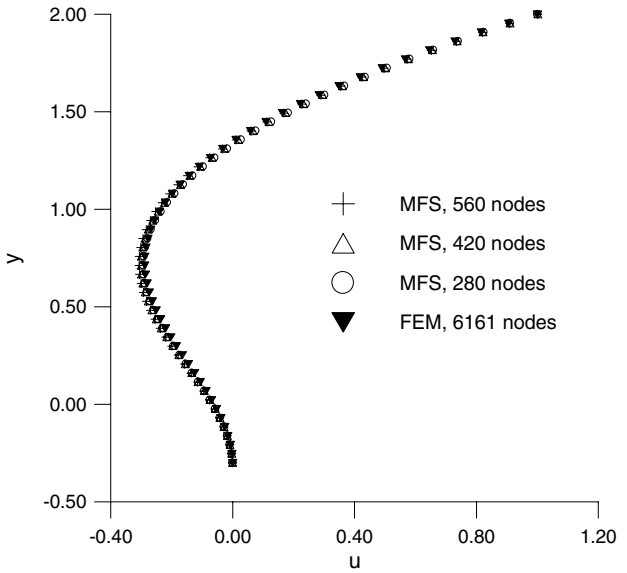

Fig. 3. Comparison of u velocity profile along y at $x = 2.5$ for a rectangular cavity with wave-shaped bottom.

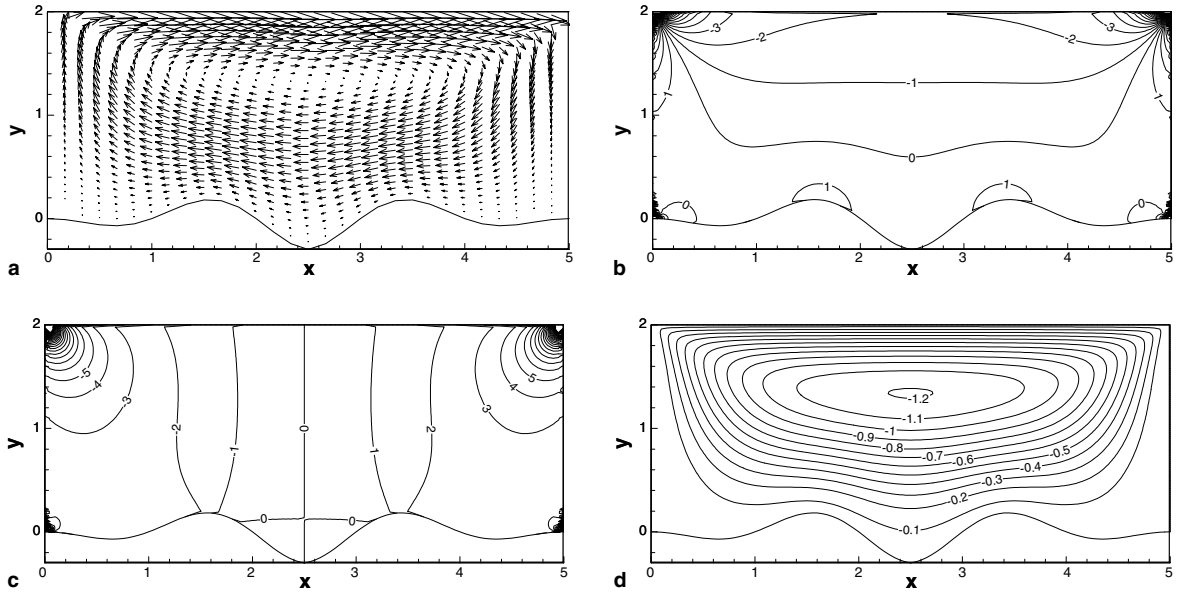

Fig. 4. (a) Velocity vector. (b) Vorticity contour ω_z. (c) Pressure contour p. (d) Streamline ψ for a rectangular cavity with wave-shaped bottom.

4.3. Cubic cavity

For the 3D application, a cubic cavity with the top lid moving with a unit velocity in the horizontal direction is considered on the Cartesian coordinate system with the x–y coordinates representing the horizontal plane and the z-coordinate directing in the vertical direction. Figs. 5(a) and (b) show the comparisons of u–z and x–w plots between the MFS solutions obtained using 150, 294 boundary field points and the results obtained by a meshless BEM [5] and the MQ method [11]. The solutions of the MFS with 294 boundary field points are in close agreement with the results of the meshless BEM [5] and MQ [11]. Figs. 6(a)–(c)

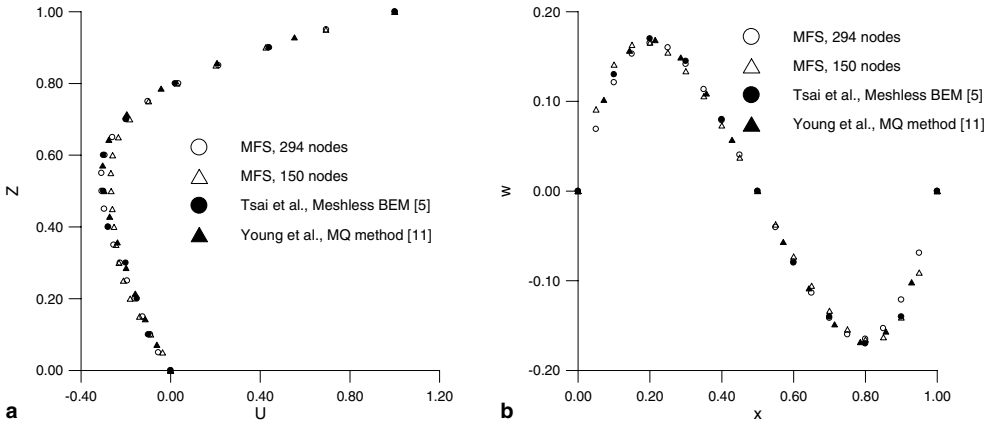

Fig. 5. Comparison of: (a) u velocity profile along z at $x = 0.5$ and $y = 0.5$ (b) w velocity profile along x at $y = 0.5$ and $z = 0.5$ for a cubic cavity.

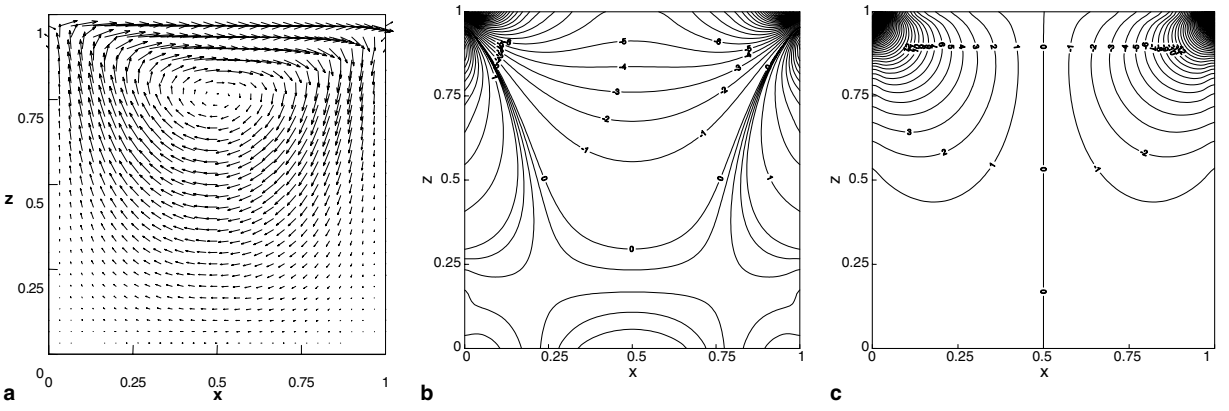

Fig. 6. (a) Velocity vector. (b) y-direction vorticity contour ω_y. (c) Pressure p contour at $y = 0.5$ plane for a cubic cavity.

illustrate the distributions of velocity vector, y-direction vorticity and pressure on x–z plane at $y = 0.5$, respectively. These figures also highlight the flow symmetry expected in the Stokes flow. In the present case the spatial parameter b in Eq. (7) is assumed to be 0.9 and the resulting matrix equations are free from the ill-conditioning effect.

5. Conclusions

The MFS has been successfully used to solve 2D and 3D Stokes equations with Stokeslets as source points. Validation results for a square cavity indicate that flow solutions close to the NSBIEM and MQ calculations could be achieved, when 80 source points are located off the boundary at about 90% of the distance from the center. For the case of a rectangular cavity with wave-shaped bottom, the proposed scheme requires only 560 boundary field points to produce flow solutions close to the FEM results obtained using 6161 grid points. For the cubic cavity, results obtained using 294 boundary nodes also show close agreement with the solutions of the meshless BEM and MQ. Thus, the MFS based on the Stokeslets is found to be a simple and computationally efficient numerical tool to solve Stokes equations in regular 2D and 3D domains and 2D irregular domain.

Acknowledgements

The National Science Council of Taiwan is gratefully acknowledged for supporting this research under the Grant Nos. NSC 93-2611-E-002-001 and NSC 94-2211-E-464-001. We are also grateful to the two anonymous referees for their constructive comments and to Prof. M.A. Golberg for helping to edit the manuscript.

References

[1] G. Fairweather, A. Karageorghis, The method of fundamental solutions for elliptic boundary value problems, Adv. Comput. Math. 9 (1998) 69.

[2] M.A. Golberg, C.S. Chen, The method of fundamental solutions for potential, Helmholtz and diffusion problems, in: M.A. Golberg (Ed.), Boundary Integral Methods: Numerical and Mathematical Aspects, WIT Press/Computational Mechanics Publications, Boston, 1998, p. 103.

[3] V.D. Kupradze, M.A. Aleksidze, The method of functional equations for the approximate solution of certain boundary value problem, Zh. Vych. Mat. 4 (4) (1964) 683.
[4] Y.S. Smyrlis, A. Karageorghis, Some aspects of the method of fundamental solutions for certain biharmonic problems, CMES 4 (2003) 535.
[5] C.C. Tsai, D.L. Young, A.H.-D. Cheng, Meshless BEM for three-dimensional Stokes flows, CMES 3 (2002) 117.
[6] C. Pozrikidis, Boundary Integral and Singularity Methods for Linearized Viscous Flow, Cambridge University Press, New York, 1992.
[7] C.J.S. Alves, A.L. Silvestre, Density results using Stokeslets and a method of fundamental solutions for the Stokes equations, Eng. Anal. Bound. Elem. 28 (2004) 1245.
[8] D.L. Young, C.W. Chen, C.M. Fan, K. Murugesan, C.C. Tsai, Method of fundamental solutions for Stokes flows in a rectangular cavity with cylinders, Euro. J. Mech. B/F (in press).
[9] C.W. Chen, D.L. Young, C.C. Tsai, K. Murugesan, The method of fundamental solutions for inverse 2D Stokes problems, Comput. Mech. (in press).
[10] C.M. Fan, D.L. Young, Analysis of the 2D Stokes flows by the non-singular boundary integral equation method, Int. Math. J. 2 (2002) 1199.
[11] D.L. Young, S.C. Jane, C.Y. Lin, C.L. Chiu, K.C. Chen, Solutions of 2D and 3D Stokes laws using multiquadrics method, Eng. Anal. Bound. Elem. 28 (2004) 1233.